On the Stationary Solution of PDE based Curve Evolution

Junyan Wang, Kapluk Chan, Yadong Wang
Nanyang Technological University
Singapore
wa0009an,eklchan,yadongwang@ntu.edu.sg

Abstract

Partial Differential Equation(PDE) based curve evolution can stop far away from the stationary solution of the corresponding Euler-Lagrange(EL) equation, which is considered as a *Pseudo-Stationary-Phenomenon*(PSP) problem in this paper. The consequence of this is early termination of evolution of the deformable curve towards desired object boundary. In this paper, we attempted to provide a solution to this problem. Our contribution is twofold. First, from the theoretical point of view, the PSP problem in PDE based curve evolution is studied and a new geometric flow called the Equilibrium Flow(EF) is proposed to address the problem. We prove that by implementing the EF and the original curve evolution flow alternatively, the stationary solution to the corresponding EL equation can be attained in general. Second, we apply our idea to a general snakes model. We show that there is the PSP problem with a general snakes model. We then solve the PSP problem by applying the derived general solution to the snake model. Experimental results on both synthetic and real images are reported in this paper to demonstrate the PSP problem and illustrate our proposed method to overcome this problem.

1 Introduction

Research on Partial Differential Equation(PDE) based curve evolution methodology for boundary detection started almost two decades ago [6]. Numerous theoretical results, algorithms and applications have been reported.[9] [4] [2] [5] [11] [12] [10].

One of the significant theoretical findings is that of Epstein and Gage [4]. They proved that the tangential velocity of the evolving curve has no influence on the geometry of the curve deformation. Mathematically, it is stated as follows[4].

Lemma 1.1 *Given the geometric flow of a curve evolution by*

$$\frac{\partial C(p,t)}{\partial t} = \alpha(C(p,t))\vec{T}(C(p,t)) + \beta(C(p,t))\vec{N}(C(p,t)) \tag{1}$$

If β does not depend on the parametrization, meaning that is a geometric intrinsic characteristic of the curve, then the image of $C(p,t)$ that satisfies Eq.(1) is identical to the

BMVC 2008 doi:10.5244/C.22.65

image of the family of curves $C(\tilde{p},t)$ that satisfies

$$\frac{\partial C(\tilde{p},t)}{\partial t} = \beta(\tilde{p},t)\vec{N}(\tilde{p},t) \tag{2}$$

This result can be considered as an evidence of the Level Set implementation of a geometric curve evolution[13] in which only the normal projection of the functional gradient is used. However it also implies that the converged solution of Eq. (2) may not necessarily be the stationary solution of Eq. (1). We call this a Pseudo-Stationary-Phenomenon (PSP) problem, because the converged curve is somewhere it is not supposed to be, i.e., it can still be a non-stationary solution of the EL equation. A possible PSP problem with gradient based curve evolution is shown in Fig. 1.

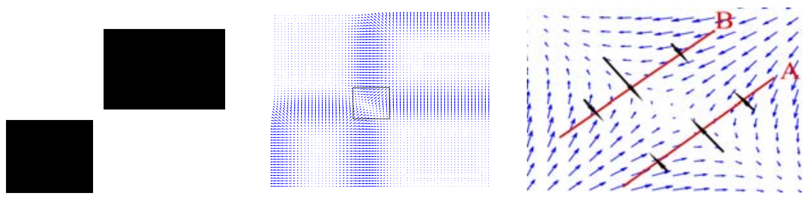

(a) A 2-D Function (b) Smoothed gradient Field of (a). (c) Oscillation of the curve evolution in the box region of (b).

Figure 1: The curve stops(or oscillates) when the gradient is nearly orthogonal to the inward normal of the curve.

Assume curves at A and B in Fig. 1(c) are from the same segment of closed curves generated by two successive iterations of some gradient driven active contour evolution. The black arrows in Fig. 1(c) denote the attraction force (caused by negative gradient) on the curves. As the curve evolves by the attraction (caused by negative gradient) drawn in Fig. 1(c), the curve at A is at first pulled towards the top-left corner to position B in the first iteration. Then, in the second iteration, the curve at B will be pulled towards bottom-right corner and towards the position A by the gradient flow. This means a gradient driven active contour cannot cross over this region but oscillate. By using a sufficiently small time step, it will finally stop at some place where the gradient is nearly orthogonal to the inward normal, but not equal to zero, which is exactly the above-mentioned PSP problem. Similar phenomena were also observed in [3] [14] [11] [12], which were not the main focus of those works. Interestingly, the scenario depicted in Figure 1, can also be considered as a saddle point problem in a gradient based optimization (see the description of this problem in[1]).

In this paper, we aim at solving the PSP problem in a general PDE based curve evolution framework. The contribution of our work is as follows.

1. Theoretically, we propose a new functional minimization procedure to ensure the stationary of the solution corresponding to the EL equation. We also derived the sufficient condition for this new functional minimization procedure, which is a PDE, called Equilibrium Flow(EF). We prove that the stationary solution is attainable by implementing the curve evolution based on the original EL equation and our proposed EF alternatively.

2. From an application point view, we derive the EF for a general snake model and show that our method, as a gradient based method, outperforms the state-of-the-art methods, e.g. Geodesic Active Contour(GAC), GAC with balloon force and GAC with adaptive balloon force, by using both synthetic and real images .

This paper is organized as follows. In section 2, we introduce the main theoretical works on the interpretation of PSP and the idea of using an Equilibrium Flow (EF) to solve a general PSP problem. In section 3, we present a case study of a general snakes model to show the PSP problem in snakes. We also derive the EF for snakes and describe the detailed algorithm. In section 4, experiments are presented to demonstrate the PSP problem and the process of our proposed method to overcome this problem.

2 The Pseudo-Stationary-Phenomenon and Equilibrium Flow

In this section, we illustrate the Pseudo-Stationary-Phenomenon(PSP) in a mathematical way and we then propose our approach to solve the PSP problem in general.

As mentioned above, Lemma 1.1 implies that there is a PSP problem with traditional PDE based curve evolution methodology. We ascertain this by a corollary below.

Corollary 2.1 *The converged curve $C(p,\infty)$ of Eq. (2),satisfying*

$$\frac{\partial C(\tilde{p},\infty)}{\partial t} = \beta(C(\tilde{p},\infty))\vec{N}(C(\tilde{p},\infty)) = 0 \tag{3}$$

may lead to

$$\begin{aligned}\frac{\partial C(p,\infty)}{\partial t} &= \alpha(C(p,\infty))\vec{T}(C(p,t\infty)) + \beta(C(p,\infty))\vec{N}(C(p,\infty)) \\ &\neq 0\end{aligned}$$

where $\alpha(C(p,\infty))$ can be large.

Since it is proven (according to Lemma 1.1) the curve evolution is independent of the tangential component of the negative functional gradient, i.e., the α in Eq. (1), the problem is inherently with a PDE based curve evolution methodology and a solution to this problem is not readily available. We propose a solution to this problem by utilizing an auxiliary geometric flow (PDE of curve evolution) named *Equilibrium Flow* which is formulated as follows.

To facilitate the following discussions , we rewrite EL-equation below w.r.t. the negative functional gradient F.

$$\frac{\partial C(p,t)}{\partial t} = \nabla\vec{F}(p,t) = \langle\vec{F}(p,t),\vec{N}(p,t)\rangle\vec{N}(p,t) + \langle\vec{F}(p,t),\vec{T}(p,t)\rangle\vec{T}(p,t) = 0 \tag{4}$$

which is essentially in the form used in Eq. (1), but by setting $\alpha = \langle\vec{F},\vec{T}\rangle$ and $\beta = \langle\vec{F},\vec{N}\rangle$.

To find the C such that $\alpha(C) = \langle\vec{F}(C),\vec{T}(C)\rangle = 0$, we propose the following functional(integral) minimization to minimize the α in Eq.(1),

$$C^* = \arg\min_C J^* = \int_0^1 |\langle\vec{F}(p,t),\vec{T}(p,t)\rangle| dp \tag{5}$$

Remark The solution $C^*(p)$ of Eq. (4) is the optimal solution of the above minimization (5) and $J^*(C^*) = 0$. If the solution of Eq. (5) is non-existence for $J^* = 0$, then there is also no solution to Eq. (4).

One can obtain the necessary optimality condition of (5), i.e., Euler-Lagrange equation, by calculating the first order variation of the functional minimization. However, we prefer a sufficient condition below.

$$\frac{\partial C(p,t)}{\partial t} = \langle \vec{F}, \vec{T} \rangle \vec{N} = 0 \tag{6}$$

Remark The solution C^* of the above equation is either an stationary solution to Eq. (10) or a level set of the original functional corresponding to the negative functional gradient $\vec{F}$.

We give the proof as follows.

Proof Since $\langle \vec{F}(C^*), \vec{T}(C^*) \rangle = 0$, we can directly obtain

$$\vec{N}(C^*) = \pm \frac{\vec{F}(C^*)}{\|\vec{F}(C^*)\|}$$

otherwise,

$$\vec{F}(C^*) = 0$$

The former equation is one of the definitions of level set, which completes the proof. ∎

We name Eq.(6) an Equilibrium Flow(EF) due to the above property of the flow. By using this EF flow, we obtain the main theoretical contribution of this paper.

Proposition 2.2 *Given an arbitrary initial curve C_0, the asymptotically converged curve $C(\tau,\infty)$ driven by following system of flows is the solution of the Euler-Lagrange equation in Eq. (1) which provides a stationary solution to the corresponding functional minimization ($\vec{F}$ is the negative functional gradient).*

$$\left\{ \begin{array}{l} \dfrac{\partial C_1^k}{\partial t} = \langle \vec{F}, \vec{N} \rangle \vec{N}, \ \ where \ \ C_1^k(\tau,0) = C_2^{k-1}(\tau,\infty) \\ \dfrac{\partial C_2^k}{\partial t} = \langle \vec{F}, \vec{T} \rangle \vec{N}, \ \ where \ \ C_2^k(\tau,0) = C_1^k(\tau,\infty) \end{array} \right. , \ k = 1, 2, \ldots \tag{7}$$

$$C_1^0(\tau,0) = C_2^0(\tau,\infty) = C_0$$
$$C(\tau,\infty) = \lim_{k\to\infty} C_1^k(\tau,\infty) = \lim_{k\to\infty} C_2^k(\tau,\infty)$$

The proof of this proposition is straightforward by using the previous propositions. However, we need to point out that the universal existence of the converged curve $\lim_{k\to\infty} C_2^k(\tau,\infty)$ has not been examined.

Besides, the curve evolution by Eq. (6) cannot be directly implemented in a level set framework where the tangent $\vec{T}$ cannot be directly used. Fortunately, in the 2D case, there is a very simple but strong relation where $\vec{N} = \mathscr{A}\vec{T}$, and $\mathscr{A}$ is a ± 90 degree rotation matrix. Therefore, we can rewrite an EF below

$$\frac{\partial C(p,t)}{\partial t} = \langle \vec{F}, \vec{T} \rangle \vec{N} = \langle \vec{F}, \mathscr{A}\vec{N} \rangle \vec{N} = \langle \mathscr{A}^T \vec{F}, \vec{N} \rangle \vec{N} = 0 \tag{8}$$

The EF can therefore be implemented directly using the level set method.

3 Solving PSP problem in curve evolution of Snakes using the Rotated Gradient Field

In this section, we apply our theoretical finding to the general snakes model[6][15]. We will show that there is the PSP problem with a general snakes model. Then we apply the previous derived general solution to the snakes to solve the corresponding PSP problem.

At first, we need to derive a compact PDE representation of snakes model. Following the derivations in [15], we can have the Euler-Lagrange equation of a general snakes model below.

$$\begin{aligned}\frac{\partial C(s,t)}{\partial t} &= \vec{F}_{int} + \vec{F}_{ext} \\ &= \alpha\kappa\vec{N} - \beta\left((\kappa_{ss} + \kappa^3)\vec{N} - 3\kappa\kappa_s\vec{T}\right) + \lambda(-\nabla g)\end{aligned} \tag{9}$$

where s, is the arc-length parametrization, $g = \frac{1}{1+|\nabla G_\sigma I|}$ is the edge indication function w.r.t. image I, κ is the mean curvature.

Due to the difficulty of computing high order difference, we normally drop the term multiplied by β, which is usurally called the rigid force term. The resultant curve evolution becomes,

$$\frac{\partial C(s,t)}{\partial t} = \alpha\kappa\vec{N} + \lambda(-\nabla g) \tag{10}$$

Notice that, if we set $\alpha = g$ and $\lambda = 1$, then the above equation turns out to be almost the same as the geometric flow of Geodesic Active Contour (GAC)[2], since the effects of the term $-\nabla g$ here and the term $-\nabla g\vec{N}$ in GAC are the same according to Lemma 1.1. This implies that the problem with Eq. (10) must also be encountered by GAC too. For this reason, we will mainly compare our proposed method with different variations of GAC.

The following shows the existence of PSP problem in traditional curve evolution implementation, e.g. splines and level sets, of Eq. (10).

Lemma 3.1 *If the curve evolution by Eq.(10) stops at C^* where $\|\alpha\kappa\| \approx 0$ at C^*, then we have either $\|\nabla g(C^*)\| \approx \vec{0}$ or $\|\nabla g(C^*)\| \gg \vec{0}$. Especially, if $\|\kappa\| = 0$ then then we have either $\|\nabla g(C^*)\| = \vec{0}$ or $\|\nabla g(C^*)\| = |\langle \nabla g(C^*), \vec{T}\rangle| \gg 0$.*

Since this lemma is not so straightforward, one can also refer to Fig. 1 for an intuitive comprehension. As already stated, driven by the negative gradient, curve A finally stops at curve B after some iterations. The gradient along the converged curve will be tangent to the curve.

Proof The stopping condition of the curve evolution by Eq.(10) can be written below.

$$\begin{aligned}&\alpha\kappa\vec{N} + \langle -\nabla g, \vec{N}\rangle\vec{N} = 0 \\ \Leftrightarrow\ &\alpha\kappa = \langle \nabla g, \vec{N}\rangle\end{aligned}$$

Given $\|\alpha\kappa\| \approx 0$, we have $|\langle \nabla g, \vec{N}\rangle| \approx 0$. Therefore, either $\|\nabla g\| \approx 0$ which proves the first half of the lemma, or$|\langle \nabla g, \vec{T}\rangle| \gg |\langle \nabla g, \vec{N}\rangle| \approx 0$.

Then, by triangular inequality

$$\|\nabla g\| \geq |\langle \nabla g, \vec{T} \rangle| - |\langle \nabla g, \vec{N}|\rangle \gg 0$$

which completes the proof(the proof for $\|\kappa\| = 0$ is similar). ∎

Roughly speaking, the curve evolution might stop when the gradient along the active contour is large and in the tangential direction of the contour, which leads an undesired scenario. This is exactly a Pseudo-Stationary-Phenomenon problem. We call it the PSP problem of snakes.

The general framework to solve the PSP problem is proposed in section 2. We can obtain the solution for PSP problem of snakes by substitution. Now we substitute the terms in Eq. (10) into Eq. (8), we will obtain the *Equilibrium Flow* for snakes as follows.

$$\frac{\partial C(p,t)}{\partial t} = \langle -\mathscr{A}^T \vec{\nabla} g, \vec{N} \rangle \vec{N} \tag{11}$$

Substituting the terms in Eq. (11) and Eq. (10) into Eq.(7), we will obtain the following geometric flows.

$$\begin{cases} \dfrac{\partial C_1^k}{\partial t} = \alpha \kappa \vec{N} + \lambda \langle -\nabla g, \vec{N} \rangle \, \vec{N} \\ \dfrac{\partial C_2^k}{\partial t} = \langle -\mathscr{A}^T \vec{\nabla} g, \vec{N} \rangle \vec{N} \end{cases}, \; k = 1, 2, \ldots, 0 < \lambda < 1 \tag{12}$$

$$\begin{aligned} &C_1^k(\tau, 0) = C_2^{k-1}(\tau, \infty), C_2^k(\tau, 0) = C_1^k(\tau, \infty) \\ &C_1^0(\tau, 0) = C_2^0(\tau, \infty) = C_0 \\ &C(\tau, \infty) = \lim_{k \to \infty} C_1^k(\tau, \infty) = \lim_{k \to \infty} C_2^k(\tau, \infty) \\ &\mathscr{A} = -\mathscr{A}^T = \begin{pmatrix} \cos \pm \frac{\pi}{2} & -\sin \pm \frac{\pi}{2} \\ \sin \pm \frac{\pi}{2} & \cos \pm \frac{\pi}{2} \end{pmatrix} \end{aligned}$$

As it follows, the Equilibrium Flow for snakes in Eq. (12) could be viewed as a gradient decent in a 90^{o} rotated gradient field. An implementation of the above idea can be an alternating application of the following two steps indicated in Eq. (12):

1. Evolve the curve in the gradient field(without rotation) by Eq. (10) until convergence.

2. Evolve the curve in the gradient field by Eq. (11) until convergence.

A consequence of the above implementation is the difficulty of defining a stopping criterion in the functional space. A practical solution to the stopping condition is by specifying a large number of iterations or comparing changes in the curve in successive alternations.

4 Experiments

In this section, we present the results of comparing our proposed method with variations of GAC, e.g. GAC[2], GAC with balloon force[2], GAC with adaptive balloon force

[11][12] while setting the parameters in our method $\alpha = g$ and $\lambda = 1$. All these geometric flows are implemented based on level set methods in [9][13][8]. ENO1 [8][13] is used for re-initialization. Realization of re-initialization are attributed to the source code in[7]. Upon preprocessing, we extend and smooth the gradient field using the Gradient Vector Flow (GVF)[14] algorithm in all our comparison experiments.

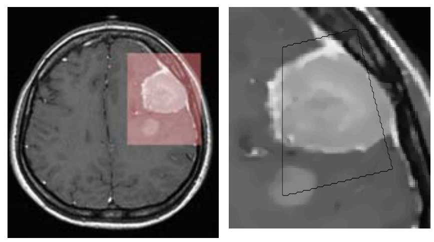

(a) Original image (b) Initialization

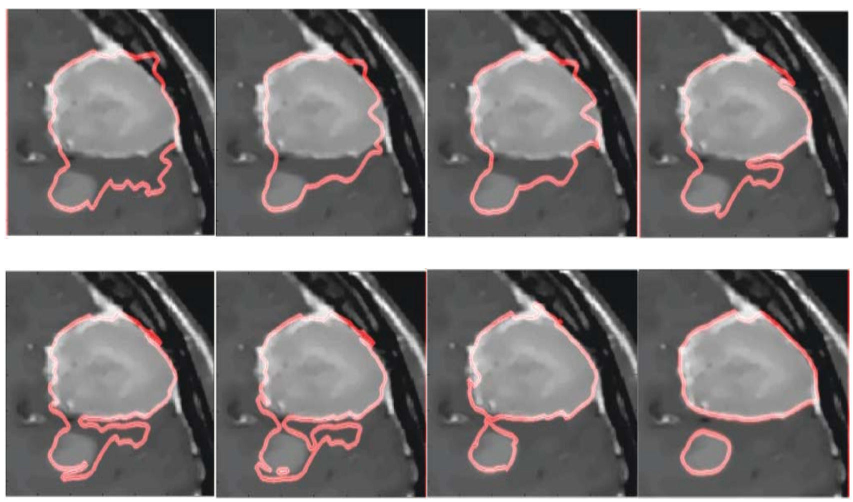

(c) Curve evolution by our proposed method

Figure 2: Our proposed method for real image (a). (b) Initial curve (marked in black) in the colour shaded region in (a). (c) Curve evolution. From left to right, top to bottom, we observe the active contour finally converges as shown in the bottom-right image in (c). Each of the images is at obtained at an interval of 100 iteration.

Experimental results for synthetic patterns are shown in Fig. 4. We run each method a maximum 5000 iterations or after observing evolution of curves has stopped. Some parts of the initial curves are placed far from desired objects or across the boundary of object. We can observe, in Fig. 4, the problem encountered by GAC and GAC with balloon force. Both of them did not fully enclose the synthetically generated patterns while GAC with adaptive balloon force achieves better results. For GAC with adaptive balloon force, the results on test pattern A is good but not for test pattern B. Comparing the above methods, our proposed method is quite successful for these synthetic image patterns.

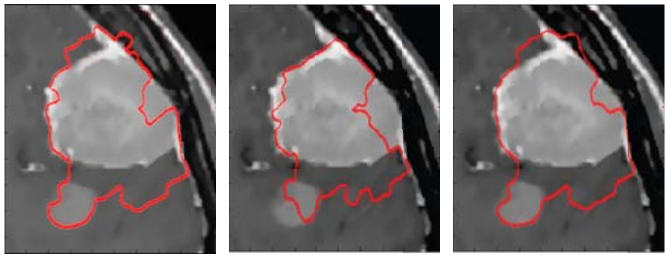

(a) GAC (b) GAC + balloon force (c) GAC + adaptive balloon force

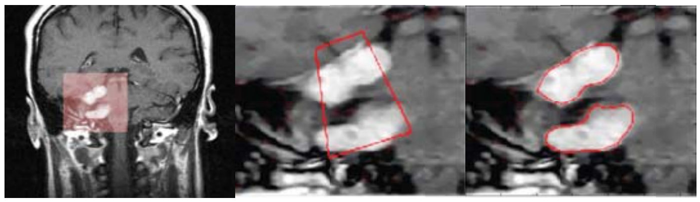

(d) Original image (e) Initialization (f) Our proposed method

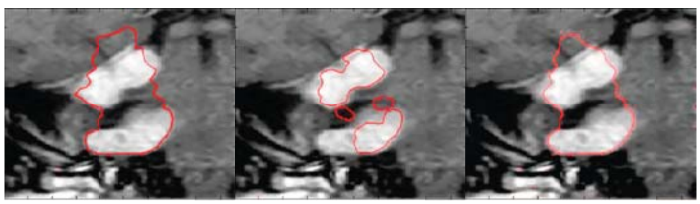

(g) GAC (h) GAC + balloon force (i) GAC + adaptive balloon force

Figure 3: The converged curve by (a) GAC; (b) GAC+balloon force; (c) GAC+adaptive balloon force; (d) The other real image;(e) is the red box region in (d) showing the initialization for all methods; (f)-(i) show the converged solutions by our method, GAC, GAC+balloon force and GAC+adaptive balloon force respectively

Real medical images are tested too. In Fig. 2 there are two tumors having different degree of contract to the non-tumor region. To enhance the information in the image, we preprocess the image by Total Variation smoothing[13] [8]. The initialization is relatively arbitrary. The results are shown in Fig. 2.

Other methods like GAC, GAC with balloon force and GAC with adaptive balloon force are also tested on image Fig.2(a) with the same initialization as in Fig.2(b). The results are shown in Fig. 3(a)-(c). We can observe that the curves cannot converge to the targeted object boundary by using all these methods. GAC is easily trapped by Pseudo-Stationary Positions in the area, while balloon force drive the curve away from the targeted boundary. The adaptive balloon force still cannot evolve the curve to the targeted boundary. Another real image is also tested that shows similar results (see Fig.3 (d)-(i)).

Finally, we also apply our algorithm to video surveillance to exactly extract interested target with an imperfect initialization. The result is shown in Fig.5.

5 Conclusion

We observe the Pseudo-Stationary-Phenomenon problem in PDE based curve evolution and provide a mathematical interpretation of the phenomenon with a general solution to this problem. The general snakes model is investigated to show that it inherently suffers from the PSP problem. The general solution is applied and the experimental results show that our proposed method outperforms the state-of-the-art methods.

References

[1] Stephen Boyd and Lieven Vandenberghe. *Convex Optimization*. Cambridge University Press, March 2004.

[2] V. Caselles, R. Kimmel, and G. Sapiro. Geodesic active contour. *International Journal of Computer Vision*, 22(1):61–79, 1997.

[3] Laurent D. Cohen. On active contour models and balloons. *CVGIP: Image Underst.*, 53(2):211–218, 1991.

[4] C.L. Epstein and Michael Gage. The curve shortening flow. Wave motion: theory, modelling, and computation, Proc. Conf. Hon. 60th Birthday P. D. Lax, Publ., Math. Sci. Res. Inst. 7, 15-59 (1987)., 1987.

[5] R. Goldenberg, R. Kimmel, E. Rivlin, and M. Rudzsky. Fast geodesic active contours. *IEEE Transactions on Image Processing*, 10(10):1467–1475, Oct 2001.

[6] M. Kass, A. Witkin, and D. Terzopoulos. Snakes: Active contour models. *International Journal of Computer Vision*, 1(4):321–331, 1988.

[7] Ian M. Mitchell and Jeremy A. Templeton. A toolbox of hamilton-jacobi solvers for analysis of nondeterministic continuous and hybrid systems. (version accepted for publication).

[8] Stanley Osher and Nikos Paragios. *Geometric Level Set Methods in Imaging,Vision,and Graphics*. Springer-Verlag New York, Inc., Secaucus, NJ, USA, 2003.

[9] Stanley Osher and James A Sethian. Fronts propagating with curvature-dependent speed: Algorithms based on Hamilton-Jacobi formulations. *Journal of Computational Physics*, 79:12–49, 1988.

[10] N. Paragios and R. Deriche. Geodesic active contours and level sets for the detection and tracking of moving objects. *Transactions on Pattern Analysis and Machine Intelligence*, 22(3):266–280, Mar 2000.

[11] N. Paragios, O. Mellina-Gottardo, and V. Ramesh. Gradient vector flow fast geodesic active contours. *Eighth IEEE International Conference on Computer Vision*, 1:67–73 vol.1, 2001.

[12] N. Paragios, O. Mellina-Gottardo, and V. Ramesh. Gradient vector flow fast geometric active contours. *IEEE Transactions on Pattern Analysis and Machine Intelligence*, 26(3):402–407, 2004.

[13] Guillermo Sapiro. *Geometric Partial Differential Equations and Image Analysis*. Cambridge University Press, New York, NY, USA, 2006.

[14] C. Xu and J. L. Prince. Snakes, shapes, and gradient vector flow. *IEEE Transactions on Image Processing*, 7(3):359–369, 1998.

[15] Chenyang Xu, Jr. Yezzi, A., and J.L. Prince. On the relationship between parametric and geometric active contours. *Signals, Systems and Computers, 2000. Conference Record of the Thirty-Fourth Asilomar Conference on*, 1:483–489 vol.1, 2000.

(a) Input images with a challenging initialization. (Left: Test pattern A; Right: Test Pattern B)

(b) Results by snakes+Balloon Force

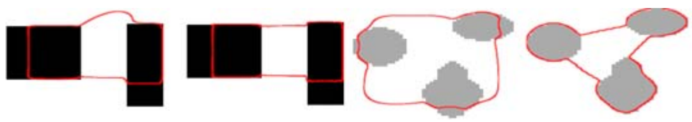

(c) Results by direct GVF+snakes

(d) Results by GVF+GAC+Adaptive Balloon Force

(e) Results by our proposed method

Figure 4: Comparison of boundary detection by variations of snakes based curve evolution with our proposed method. In (a), two test patterns, A and B, are shown with initial curves. From (b)-(e), in each row, the results are shown in the following order : intermediate stage of curve evolution on pattern A, curve upon convergence on pattern A, intermediate stage of curve evolution on pattern B, and curve upon convergence on pattern B .

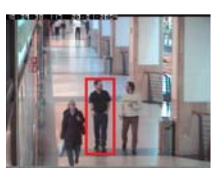

(a) Surveillance snapshot with an initial curve

(b) Room in result of object extraction

Figure 5: An application of our proposed algorithm in video surveillance is shown here.